Relationship between Availability of NMDA Receptor Subunits and Their Expression at the Synapse

Kate Prybylowski,[1] Zhanyan Fu,[2] Gabriele Losi,[2] Lynda M. Hawkins,[1] JianHong Luo,[2] Kai Chang,[1] Robert J. Wenthold,[1] and Stefano Vicini[2]

[1]*Laboratory of Neurochemistry, National Institute on Deafness and Other Communication Disorders, National Institutes of Health, Bethesda, Maryland 20892, and* [2]*Department of Physiology and Biophysics, Georgetown University Medical Center, Washington, DC 20057*

The effect of increasing the expression of NMDA subunits in cerebellar granule cells (CGCs) by transfection was studied to determine how the availability of various NMDA subunits controls both the total pool of functional receptors and the synaptic pool. Overexpression of either NR2A or NR2B, but not splice variants of NR1, by transfection caused a significant increase in the total number of functional NMDA receptors and in surface NR1 subunit cluster density in CGCs in primary culture. These data solidify the central role of NR2 subunit availability in determining the number of cell surface receptors. Overexpression of either NR2A or NR2B significantly altered the deactivation kinetics of NMDA-mediated miniature EPSCs (NMDA-mEPSCs). However, there was no significant effect of NR2 subunit overexpression on the mEPSC amplitude or single-channel conductance. NR2 subunit overexpression did not change the rate of block by MK-801 of NMDA-mediated currents in excised patches from CGCs, indicating that subunit composition does not regulate peak open probability of the channel in CGCs. With the overexpression of a mutant of NR2B lacking the PDZ binding domain, there was an increase in the total number of NMDA receptors without a change in mEPSC kinetics. Therefore, the entry of NMDA receptors into the synapse requires a PDZ binding domain and is limited by means other than receptor subunit availability.

Key words: cerebellar granule cells; ifenprodil sensitivity; NMDA-mEPSCs; peak open probability; PDZ binding domain; receptor targeting

Ionotropic glutamate receptors mediate most excitatory neurotransmission in the mammalian CNS (Dingledine et al., 1999). The number and composition of receptors on the postsynaptic membrane determine the nature and strength of the response to released neurotransmitter. Recent studies have shown use-dependent downregulation of NMDA receptors (NMDARs) (Vissel et al., 2001) as well as phosphorylation-dependent redistribution of receptors in oocytes, cultured hippocampal neurons, and striatal slices (Crump et al., 2001; Dunah and Standaert, 2001; Lan et al., 2001) and internalization via a clathrin-mediated process (Roche et al., 2001). Together, these studies suggest that NMDARs on the cell surface may be regulated via a process involving vesicular trafficking and intracellular receptor pools.

Functional NMDARs are heteromeric complexes containing NR1 and NR2 (NR2A–NR2D) subunits and possibly the NR3A subunit (Dingledine et al., 1999), with the NR2 subunit determining many functional properties of the receptor in heterologous systems (Cull-Candy et al., 2001). Expression of the NR2A subunit produces channels with comparatively rapid deactivation, whereas the NR2B subunit confers slower kinetics and sensitivity to subunit-selective antagonists (Dingledine et al., 1999). In the rat CNS there is a developmental decrease in expression of the NR2B subunit and there is an increase in expression of the NR2A subunit, both of which occur in parallel with changes in functional properties of NMDA-mediated currents (Cull-Candy et al., 2001).

The C termini of NR2 subunits of NMDA receptor can interact with the PDZ domains of membrane-associated guanylate kinases (MAGUKs), which include postsynaptic density-95 (PSD-95), PSD-93, and synapse-associated protein (SAP102) (for review, see Garner et al., 2000; Sheng, 2001; Tomita et al., 2001). It appears that MAGUKs, which are linked to a number of other postsynaptic proteins, mediate interactions with signal transduction molecules and may function to retain NMDA receptors at synapses (Kennedy, 1998). The C terminus of NR2 subunits also has been implicated in controlling the endocytosis rate (Roche et al., 2001). Truncation of large regions of the NR2A C terminus in transgenic mice causes a loss of synaptic enrichment of the NR2A subunit and the appearance of NMDA EPSCs with smaller amplitudes and slower kinetics (Steigerwald et al., 2000), indicating that the C terminus of NR2 subunits may be critical for normal subunit localization. NMDA receptors also occur outside of the synapse, but the relationship of these extrasynaptic receptors to synaptic receptors is not clear (Stocca and Vicini, 1998; Rumbaugh and Vicini, 1999; Tovar and Westbrook, 1999; Sinor et al., 2000), although recent data indicate that there may be rapid movement of receptors between synaptic and extrasynaptic sites (Tovar and Westbrook, 2002).

In the present study we investigated the relationship between total expression levels of NMDAR subunits and the number of functional NMDARs at synaptic sites. We took advantage of the

Received June 26, 2002; revised July 24, 2002; accepted July 26, 2002.

This work was supported by the Pharmacology Research Associate Program (K.P.), the National Institute on Deafness and Other Communication Disorders Intramural Program (K.P., L.H., K.C., and R.J.W.), and National Institute of Mental Health Grants MH58946 and MH01680 (S.V.). We thank Dr. L. Chen for helpful advice on culture procedures. We are grateful to Anne Stephenson for the gift of the NR2B-Flag construct.

Correspondence should be addressed to Kate Prybylowski, Laboratory of Neurochemistry, National Institute on Deafness and Other Communication Disorders, National Institutes of Health, Building 50, Room 4140, Bethesda, MD 20892. E-mail: prybylow@nidcd.nih.gov.

granule cell culture, which provides a homogenous neuronal population from which the synaptic and total receptor pools can be measured and in which NMDA receptor subunits can be overexpressed. Our results show that the increased expression of NR1 and NR2 subunits affects the production of functional NMDARs in different ways and that synaptic and total NMDARs are regulated by distinct mechanisms.

MATERIALS AND METHODS

Cerebellar granule cells culture. Primary cultures of rat cerebellar granule neurons were prepared from postnatal day 7 (P7) Sprague Dawley rat cerebella (Corsi et al., 1998). Cells were dispersed with trypsin (0.25 mg/ml; Sigma, St. Louis, MO) and plated at a density of 1.1×10^6 cells/ml on glass coverslips (Fisher Scientific, Pittsburgh, PA) coated with poly-L-lysine (10 μg/ml; Sigma) in 35 mm Nunc dishes. Cells were cultured in basal Eagle's medium supplemented with 10% bovine calf serum, 2 mM glutamine, and 100 μg/ml gentamycin (all from Invitrogen, Carlsbad, CA) and were maintained at 37°C in 6% CO_2. The final concentration of KCl in the culture medium was adjusted to 25 mM (high K^+). At 4 d *in vitro* (DIV4) cytosine arabinofuranoside (10 μM; Sigma) was added to all cultures to inhibit glial proliferation. Some cells were kept in 25 mM K^+ to block the formation of functional synapses; for parallel experiments cortical tissue from P1 rats was plated under the same conditions at a density of 1×10^6 cells/ml. To achieve functional synapse formation, at DIV4 we replaced the medium with low (5 mM) potassium medium (MEM supplemented with 5 mg/ml glucose, 0.1 mg/ml transferrin, 0.025 mg/ml insulin, 2 mM glutamine, and 20 μg/ml gentamycin; Invitrogen) as described previously by Chen et al. (2000). Recordings were made from DIV6–8 neurons in culture when there was spontaneous synaptic activity.

DNA constructs. The NR2B-Flag (NR2B subunit tagged at the N terminus with Flag epitope) has been described previously by Hawkins et al. (1999) and was a generous gift from Dr. Anne Stephenson (University College, London, UK). The Flag epitope was positioned between amino acids 53 and 54 of the NR2B subunit. The position of the tag was confirmed by DNA sequencing. The cDNA encoding NR2B-Flag subunits was subcloned into the mammalian expression vector pCIS for transfection into neurons and human embryonic kidney (HEK) 293 cells. NR2B-FlagΔ7, a mutant of NR2B-Flag that lacked the PDZ interacting domain, was made by using site-directed mutagenesis (QuikChange site-directed mutagenesis kit; Stratagene, La Jolla, CA) and by using NR2B-Flag as the template. A stop codon was introduced at position 1475, causing a loss of the last seven amino acids. The construct was verified by DNA sequencing.

NR1-1a tagged with yellow fluorescent protein (YFP) at its N terminus (NR1-1a-YFP) was constructed by inserting YFP cDNA in frame with NR1-1a cDNA between the third and fourth codons after the predicted sequence for the signal peptide. cDNA encoding YFP was amplified from plasmid pEYFP-N1 (Clontech, Palo Alto, CA). Western blot analysis indicated that NR1-1a-YFP was expressed in HEK 293 cells as an NR1-positive band at ~140 kDa, which is the expected molecular weight of a chimera of NR1 (113 kDa) and YFP (27 kDa) (data not shown). The expressional vector for NR2A-YFP was constructed by inserting a YFP cDNA fragment in frame with the NR2A subunit between the fifth and sixth codons, and Western blot analysis of transfected HEK 293 cells showed the expected increase in molecular weight of NR2A (data not shown). Coexpression of NR1-1a-YFP together with the NR2A subunit in HEK 293 cells produced functional NMDA channels (data not shown).

Cerebellar granule cell transfection. Using a modification of the calcium phosphate precipitation technique (Chen and Okayama, 1987), we transfected primary cultures of rat cerebellar granule cells (CGCs) and cortical neurons. Briefly, cultured neurons at DIV5 on a glass coverslip were transferred to a well in a four-well plate with 500 μl of transfection medium, a MEM medium (catalog number 12370-037; Invitrogen) pH-adjusted to 7.85 by 5 M NaOH. Then 30 μl of a DNA/Ca^{2+} mixture containing 3 μg of cDNAs was added and incubated for 30 min at room temperature. After two washes with the transfection medium the original culture medium was returned, and the neurons were maintained at 37°C in 5% CO_2. Enhanced green fluorescent protein (EGFP) plasmid (Clontech) also was transfected to allow for visualization of successfully transfected cells. For cells that were used for NMDA application, each coverslip was transfected with 0.3 μg of GFP plasmid and 1 μg of all NMDA subunits. Untagged NR1 and NR2 constructs were described previously (Vicini et al., 1998). If cells were transfected with only one NMDA subunit, 1 μg of plasmid DNA for NR2A in pBluescript (containing a bacterial promoter) was used to control for equal amounts of DNA for each transfection.

Immunocytochemistry. Cultured CGCs were transfected with NR1-1a tagged with YFP at the extracellular N terminus (NR1-1a-YFP) alone or with NR2A or NR2B. YFP fluorescence was undetectable on the dendrites of transfected neurons, so a surface-staining protocol with antibody staining of live neurons with anti-GFP antibody was used specifically to assess the surface expression of NR1-1a-YFP. CGCs were incubated with polyclonal antibodies against GFP (Chemicon, Temecula, CA; recognizes YFP) at 2 μg/ml in extracellular medium (recipe below) for 6 min at room temperature. After three PBS washes the cells were incubated with Alexa 488-conjugated anti-rabbit antibody (Molecular Probes, Eugene, OR) at 1:400 for 6 min. Then the cultures were fixed with paraformaldehyde and were imaged. Neurons were imaged on a Nikon EN600 microscope equipped with a 60×, 1.0 numerical aperture objective. The camera is a Hamamatsu Orca-100, 12-bit cooled CCD digital camera, 1392×1040 pixel array, 6.45×6.45 μm pixel size. Images were captured and pseudocolored for presentation by the use of MetaMorph imaging software (Universal Imaging, Downingtown, PA) and Adobe Photoshop 6.0. For measurements of synaptic colocalization, after surface staining with anti-GFP antibody the CGCs were fixed with methanol and permeabilized with 0.25% Triton X-100; staining was done with anti-synaptophysin antibody (1:1000 dilution; Boehringer Mannheim, Mannheim, Germany), followed by secondary antibody staining with indocarbocyanine (Cy3)-labeled goat anti-mouse antibody (Jackson ImmunoResearch, West Grove, PA). Antibody-positive receptor clusters were defined as clusters of fluorescence that were at least twice the background fluorescence of the image. Colocalization of YFP and synaptophysin-positive puncta was defined as having overlapping pixels. All immunocytochemical analysis was done blinded.

For fixed cell immunocytochemistry to determine subunit overexpression, we performed all antibody and incubations for staining experiments at room temperature. Cultured CGCs were fixed in 4% paraformaldehyde/4% sucrose in PBS for 5 min and then were incubated in 0.025% Triton X-100 for 3 min. Cells were preincubated in 10% BSA (Sigma) for 1 hr and then incubated in primary antibodies in PBS containing 3% BSA for 1 hr. Monoclonal antibody against NR1 subunit (Luo et al., 1997) was used at 1 μg/ml. Rabbit anti-NR2B and NR2A subunits (Chemicon) were used at 1:400. After being washed with PBS for several times, the cells were incubated with secondary antibodies for 1 hr. Both Cy3-conjugated goat anti-mouse and anti-rabbit IgG antibodies (Jackson ImmunoResearch) were used at 1:2000. Coverslips were mounted on slides with Antifade component A (Molecular Probes) as a mounting medium.

Solutions and drugs. The recording chamber was perfused continuously at 5 ml/min with an extracellular medium composed of (in mM): 145 NaCl, 5 KCl, 1 $MgCl_2$, 1 $CaCl_2$, 5 HEPES, 5 glucose, and 25 sucrose plus 0.25 mg/l phenol red and 20 μM D-serine (all from Sigma). Successfully transfected cells were visualized by using GFP fluorescence as a marker. Cells were used DIV5–7, which was 1–2 d after transfection. CGCs were voltage clamped at −60 mV, and a potassium gluconate recording solution was used containing (in mM): 145 potassium gluconate, 10 HEPES, 5 ATP-Mg, 0.2 GTP-Na, and 10 BAPTA, pH-adjusted to 7.2 with KOH. NMDA (200 μM) in Mg^{2+}-free perfusion solution (with 1 μM TTX to block possible synaptic responses stimulated by NMDA) was applied to CGCs via a gravity-fed Y-tubing system to stimulate all cell surface receptors (Murase et al., 1989). Ifenprodil (Sigma) was coapplied with NMDA. Recording electrodes were pulled in two stages on a vertical pipette puller from borosilicate glass capillaries (Wiretrol II; Drummond, Broomall, PA). Typical pipette resistance was 5–7 MΩ. Whole-cell recordings were performed with a patch-clamp amplifier (Axopatch 200; Axon Instruments, Foster City, CA). Experiments with HEK 293 cell transfection were done by using the protocols of Vicini et al. (1998).

Synaptic recordings. CGCs switched to low potassium at DIV4 began to show synaptic NMDA currents at DIV6. CGC recording at +60 mV were made from DIV6–8 cells with a Cs-methanesulfonate recording solution that blocks voltage-dependent potassium currents containing (in mM): 145 Cs-methanesulfonate, 10 BAPTA, 5 $MgCl_2$, 5.0 ATP-Na, 0.2 GTP-Na, and 10 HEPES, pH-adjusted to 7.2 with CsOH. Via Y-tubing a perfusion solution with 1 mM Mg^{2+} and 50 μM bicuculline (Sigma) was applied to the cell being recorded. Cells were held initially at −60 mV, and then the holding voltage was jumped to +60 mV to relieve the Mg^{2+}

block of the NMDA receptor. All experiments were performed at room temperature (24–26°C). Experiments also were done to record miniature NMDA-EPSCs at −60 mV in Mg^{2+}-free solution. These recordings were done with K-gluconate solution (described above) in the presence of 1 μM TTX, 5 μM NBQX, and 50 μM bicuculline. Single-channel current amplitude estimates from the tails of synaptic currents were analyzed by using the Fetchan and pStat routines of the pClamp 6.03 software suite. Rare openings at subconductance levels were excluded from the amplitude analysis.

MK-801 blockade. Nucleated patches were pulled from transfected and control neurons. Then patches were placed in the flow of the piezo-driven (P-245.30 Stacked Translator; Physik Instrumente, Waldbronn, Germany) double-barrel pipette by following the procedure described by Vicini et al. (1998). Control solution contained 0.2 mM $CaCl_2$ (to minimize rundown of the response over repeated agonist applications), 5 μM NBQX (to block AMPA responses), and 20 μM D-serine in Mg^{2+}-free solution. Then 4 msec jumps were made to a solution that also contained 1 mM glutamate. After the baseline response was measured, the glutamate solution was exchanged for a solution with 1 mM glutamate and 20 μM MK-801 (glutamate/MK-801). Repeated applications then were made of glutamate/MK-801, and the amplitude and kinetics of the responses were measured.

Data collection and analysis. Currents were filtered at 1 kHz with an eight-pole low-pass Bessel filter (Frequency Devices, Haverhill, MA) and digitized at 5–10 kHz by using an IBM-compatible microcomputer equipped with Digidata 1200 data acquisition board and pClamp 8 software (both from Axon Instruments). Off-line data analysis, curve fitting, and figure preparation were performed with Clampfit 8 (Axon Instruments), Origin 4.1 (Microcal, Northampton, MA), and Mini Analysis (Synaptosoft, Decatur, GA) software. Fitting of the decay phase of currents recorded from granule cells in culture was performed by using a simplex algorithm for least squares exponential fitting routines. Decay times of averaged currents were derived from fitting to double-exponential equations of the form: $I(t) = I_f \times \exp(-t/\tau_f) + I_s \times \exp(-t/\tau_s)$, where I_f and I_s are the amplitudes of the fast and slow decay components, and τ_f and τ_s are their respective decay time constants used to fit the data. To compare decay time between different subunit combinations, we used a weighted mean decay time constant: $\tau_w = [I_f/(I_f + I_s)] \times t_f + [I_s/(I_f + I_s)] \times t_s$. Data values are expressed as the means ± SEM unless otherwise indicated. *p* values represent the results of ANOVA analysis, with $p < 0.05$ being defined as the level for significance.

RESULTS

The availability of NR2 subunits determines the total number of functional NMDA receptors in cerebellar granule cells

Because a complex containing both NR1 and NR2 subunits is required for a functional NMDA receptor, the availability of either subunit could limit the production of functional receptors in neurons. To determine whether either NR1 or NR2 is limiting in granule cells, we increased the amount of available subunit by transfecting neurons with GFP and either NR1 or NR2 cDNAs. These CGCs were plated in 25 mM K^+ and then switched to 5 mM K^+, using a medium that has been shown to allow for the formation of functional synapses (Chen et al., 2000). Successfully transfected CGCs were visualized via GFP fluorescence. Using local application with Y-tubing, we measured the peak response to 200 μM NMDA (together with 1 μM TTX to block synaptic inputs). D-Serine (20 μM) also was included in the solution to saturate the glycine site on the NMDA receptor and to avoid activation of the glycine receptor chloride channel. The amplitude of response to this NMDA application was what we defined as the total number of NMDA receptors, which would include receptors localized to synaptic sites and those at extrasynaptic sites. At 1–2 d after transfection there was no effect of overexpression on peak response to NMDA with either NR1-1a or NR1-4a cDNA splice variants in comparison with untransfected neurons (Fig. 1*A,B*). In addition, we also tested the response to NMDA by using an NR1a subunit with an N-terminus tag (NR1a-YFP), which allowed us to visualize transfected neurons based directly on expression of the tagged subunit. NR1a-YFP-transfected neurons did not show a change in current density compared with control (current density = 47 ± 10 pA/pF; $n = 6$ cells). On the other hand, after transfection with either NR2A or NR2B there was a significant increase in the amplitude of response to NMDA (Fig. 1*B*; $p < 0.01$).

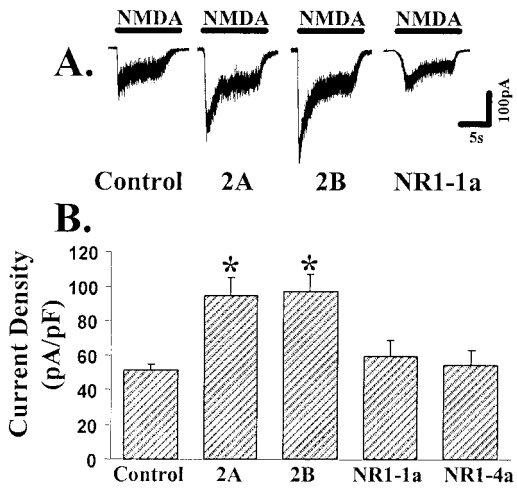

Figure 1. Effect of NMDA subunit overexpression on NMDA-mediated currents in CGCs in culture. *A*, Representative traces from control CGCs or CGCs that were transfected with cDNAs for subunits of the NMDA receptor and the fluorescent marker GFP. CGCs were cultured in 5 mM K^+, and successfully transfected cells were determined by GFP fluorescence. Whole-cell recordings were done 48 hr after transfection with the application of 200 μM NMDA and 20 μM D-serine with 1 μM TTX in nominally Mg^{2+}-free solution via a Y-tubing system. *B*, Summary of current density responses from multiple CGCs (at least 6 cells in each group). Transfection with NR1-1a or NR1-4a did not cause a significant change in the current density compared with control (ANOVA). Transfection with NR2A or NR2B caused a significant increase in current density (*$p < 0.01$).

Table 1. NMDA-mediated currents in transfected neurons

CGCs in high K^+		Cortical neurons	
Control	40.7 ± 3.2	Control	15.3 ± 4.0
NR1-1a	31.5 ± 3.7	NR1-4b	16.6 ± 3.3
NR1-4a	34.7 ± 10.5	2A	34.7 ± 5.2*
GFP	33.2 ± 1.7	2B	27.4 ± 3.2*
2A	59.7 ± 8.0*	2B+NR1-1a	47.7 ± 9.3*
2B	78.7 ± 8.8*		
2B+NR1-4b	95.2 ± 20.2*		
2B+NR1-1a	99.9 ± 15.5*		

Values are in current density (pA/pF). CGCs were cultured in 25 mM K^+ and cultured cortical neurons were from P1 rats. *$p < 0.05$ versus control. $n > 6$ cells for each group.

NMDA subunit overexpression also was tested in CGCs plated in 25 mM K^+, which has been shown to block the formation of functional synapses (Mellor et al., 1998). A similar effect of NR2 subunits to increase current density was seen with the overexpression of NR2, but not NR1, subunits in the absence of synaptic activity (Table 1). In addition, similar results were seen in cortical neurons. These data indicate that the effect of NR2 subunit overexpression is not dependent on synaptic activity or culture conditions, and it is not restricted to CGCs.

We also studied the effect of subunit overexpression on the

ability of NMDA responses to be antagonized by ifenprodil, an antagonist that is specific for NR1/NR2B receptors (Williams, 1993). As reported previously in untransfected CGCs neurons (Corsi et al., 1998), the application of 10 μM ifenprodil reduced NMDA current density by 50.5 ± 8.2% (n = 9). NR2A-transfected neurons showed significantly less reduction in current density in the presence of ifenprodil (27.5 ± 5.0%), and NR2B-transfected neurons showed more reduction (68.9 ± 3.3%).

Immunocytochemical data indicate increased NR1 surface expression in NR2 subunit-transfected CGCs

Immunocytochemistry also was done to confirm subunit overexpression by using antibodies that are specific for the NR1, NR2A, and NR2B subunits. Overexpression of NR1 splice variants, NR2A, and NR2B was confirmed by using permeabilized antibody staining with subunit-specific antibody, which showed increased expression of all transfected subunits compared with untransfected neurons in the same field (data not shown). In addition, the surface expression of the NMDAR subunits was tested by using epitope-tagged constructs containing epitope tags on their extracellular N terminus (NR1-1a-YFP, NR2A-YFP, and NR2B-Flag; construct design is outlined in Materials and Methods). Although none of these constructs showed surface staining when transfected alone in HEK 293 cells, surface staining in CGCs could be seen for all of these constructs, indicating that transfected subunits could coassemble with corresponding endogenous subunit partners because unassembled NR2 subunits and NR1-1a are endoplasmic reticulum-retained in the absence of partner subunits (McIlhinney et al., 1998; Standley et al., 2000). The ability of NR1-1a-YFP to be surface-labeled in CGCs allowed us to confirm our measurement of changes in the number of functional NMDA receptors after NR2 subunit overexpression that were seen by using NMDA application. NR1-1a-YFP was transfected into CGCs and allowed for the visualization of synaptic puncta with the surface-staining protocol (Fig. 2*A*), indicating that NR1-1a-YFP was able to enter the pool of total NR1, assemble with NR2 subunits, and form surface puncta. In double-blind experiments the staining with anti-GFP antibody was done on live neurons, and the number of GFP-positive puncta was measured per unit of dendrite in NR1-1a-YFP alone transfected and in cotransfections with either NR2A or NR2B subunits (Fig. 2). Staining was done either on live cells as shown or after mild paraformaldehyde fixation; puncta were similar in both cases, indicating that labeling was specific for receptor clusters and was not an artifact of antibody clustering of receptor proteins. The number of clusters per unit of dendrite was measured, and a significant increase in the number of antibody-labeled receptor puncta was seen with the cotransfection with NR2A and NR2B (Fig. 2), although the amount of NR1-1a-YFP cDNA that was transfected was constant over experiments (see Materials and Methods). These data confirm that the overexpression of NR2 subunits is able to recruit more NR1 subunit protein to the surface in receptor complexes. In addition, experiments were done to study the percentage of YFP-positive puncta that were colocalized with synaptophysin, a marker of presynaptic terminals (Fig. 2). In this case the percentage of total YFP-positive puncta that were colocalized with synaptophysin was reduced for NR2A and NR2B, indicating a preference for the new receptors formed with the overexpression of NR2 subunits to be located extrasynaptically.

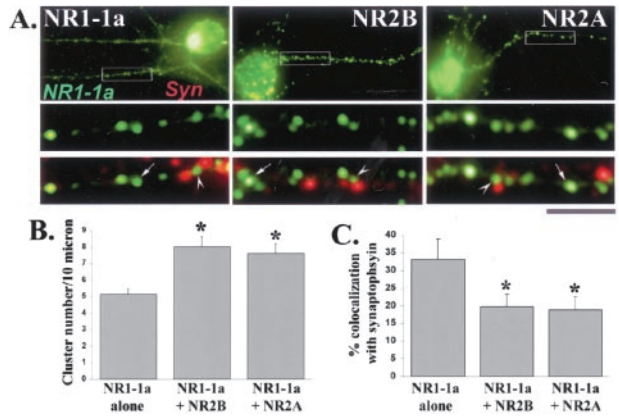

Figure 2. Transfection with cDNAs for NR2 subunits causes increased extrasynaptic surface NR1 clusters. *A*, CGCs were transfected with cDNAs for NR1-1a-YFP alone or with NR2A or NR2B on parallel coverslips to those used in the experiments outlined in Figure 1. Surface expression of NR1-1a-YFP was measured with anti-GFP antibody staining (shown in *green*), followed by permeabilization and staining with anti-synaptophysin staining (shown in *red*). The *top row* shows low-power micrograph of surface NR1-1a-YFP staining for CGCs that were transfected in different conditions. *Insets*, Partial segments of dendrites with anti-YFP staining (in *green*) and their merged images with anti-synaptophysin staining (in *red*). *Arrowheads* in the *insets* indicate examples of synaptic clusters; *arrows* indicate examples of unmatching clusters. Scale bar: 15 μm; for *insets*, 3.6 μm. *B*, The number of NR1-1a-YFP-labeled clusters per 10 μm of dendritic length averaged for several fields of one dendrite in each cell from at least 20 individual cells for each group. *Statistically significant from the value in control cells ($p < 0.05$). *C*, The percentage of colocalization of NR1-1a-YFP-labeled clusters with synaptophysin staining (from at least 10 individual cells). *Statistically significant from the value in control cells ($p < 0.05$).

NR2 subunit expression alters kinetic properties of synaptic currents, but not the amplitude

CGCs were used as a model for studying the effect of the transfection of NMDA subunits on synaptic NMDA receptors, because they are highly presynaptically and postsynaptically homogenous (Gallo et al., 1987). CGCs initially were plated in high K^+ (25 mM) and switched in low K^+ medium (5 mM) at DIV4 to promote functional synapses while maintaining healthy neurons. Neurons were recorded from DIV6–8 at 2–3 d after transfection with NMDA subunits. CGCs were recorded in 1 mM Mg^{2+}-containing recording solution with 50 μM bicuculline and were held at +60 mV, with NMDA-mediated slow EPSCs (NMDA-EPSCs) being seen as outward currents. Overlapping NMDA-EPSCs were excluded from analysis, although this was a rare occurrence given the low frequency of NMDA-EPSCs. Most CGCs grown in these conditions showed NMDA-EPSCs, and individual cells showed very similar NMDA-EPSC properties. The slow currents seen at +60 mV were blocked totally by 30 μM CPP (data not shown), indicating that the sEPSCs that were measured were solely NMDA mediated.

Traces of responses from individual neurons are shown in Figure 3*A*, and representative averaged traces from control and transfected neurons are shown in Figure 3*B*. These averaged traces are from at least 15 individual NMDA-EPSCs from a single CGC. The averaged spontaneous NMDA-EPSCs amplitude and deactivation kinetics are summarized in Figure 3, *C* and *D*. The frequency of occurrence of NMDA-EPSCs at room temperature in control CGCs (n = 32) was 0.13 ± 0.01 Hz, and it was not changed significantly by the cotransfection of any subunit.

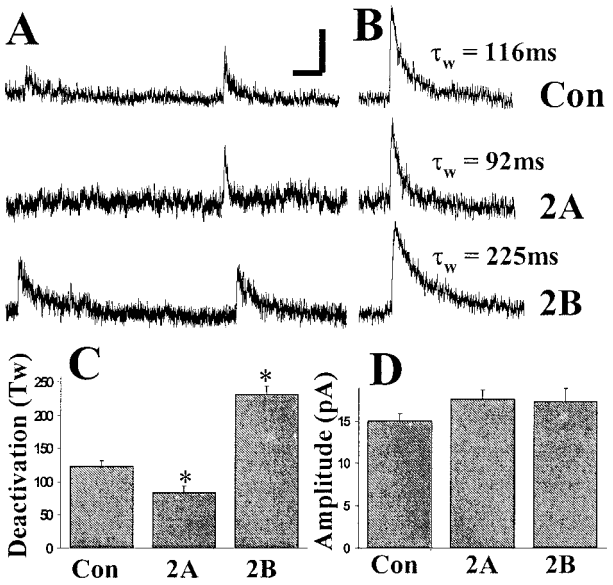

Figure 3. Effect of overexpression of NR2 subunits on NMDA-EPSC characteristics in CGCs. CGCs were transfected with either NR2A or NR2B, and NMDA-EPSCs were recorded from control or transfected cells cultured in 5 mM K^+ medium (see Materials and Methods). Recordings were made in extracellular solution with 1 mM Mg^{2+} at +60 mV with Cs-methanesulfonate recording solution and with 50 μM bicuculline applied to the CGC being recorded via Y-tubing. *A*, Representative recording traces of sEPSCs from CGCs. Calibration: 500 msec, 10 pA. *B*, Averaged sEPSCs together with an indication of the weighted time constant of decay (τ_w) from an individual CGC. Calibration: 125 msec, 7 pA. *C*, Averaged τ_w for deactivation kinetics. *D*, sEPSC amplitude from at least 20 individual cells for each group. *Statistically significant from the value in control cells ($p < 0.05$).

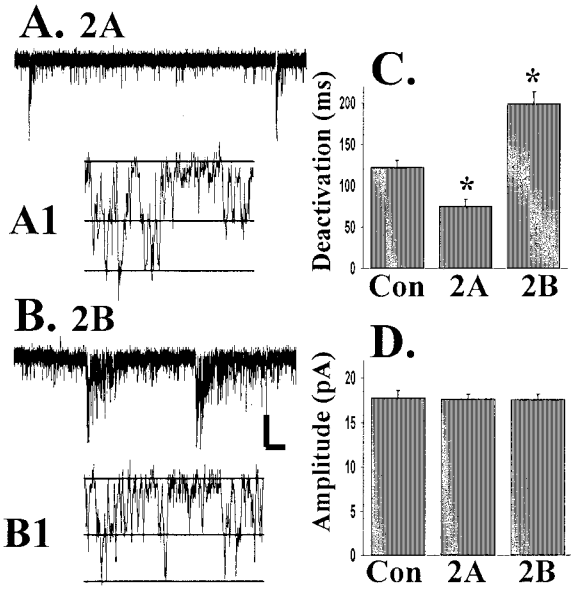

Figure 4. NR2 subunit expression controls the deactivation kinetics of NMDA-mEPSCs, but not the mEPSC amplitude or the single-channel conductance. NMDA-mEPSCs were recorded at −60 mV in the presence of bicuculline (50 μM), TTX (1 μM), and NBQX (5 μM). *A*, Representative NMDA-mEPSCs from an NR2A-transfected neuron. *A1*, Channel opening in the tail of a mEPSC, with the *line* on the trace indicating overlapping open channel currents. *B, B1*, Similar data for an NR2B-transfected CGC. *C*, Averaged data (from at least 6 cells in each group) measuring the deactivation kinetics of NMDA-mEPSCs that were significantly different after transfection of either NR2A or NR2B (*$p < 0.01$). *D*, There was no significant difference in NMDA-mEPSC amplitude. Calibration: *A, B*, 0.5 sec, 5 pA; *A1, B1*, 4 msec, 4 pA.

With transfection of the NR2A subunit the NMDA-EPSCs deactivation kinetics were significantly faster than control, and with overexpression of the NR2B subunit the NMDA-EPSC deactivation kinetics were slower than control (Fig. 3*C*; $p < 0.05$; *n* of at least 20 neurons). For both NR2A and NR2B transfections there was no statistically significant change in NMDA-EPSC amplitude with transfection. With cotransfection of the NR1-4b subunit (5 cells; data not shown) the amplitude and deactivation kinetics were not different from control (amplitude, 16 ± 4 and τ_w, 129 ± 23).

To rule out any effect of AMPA currents, we also recorded miniature NMDA-EPSCs (mEPSCs) at −60 mV in the presence of bicuculline, TTX, and NBQX as shown in Figure 4. Recordings at negative potentials were characterized by a considerably lower background noise. This allowed for the observation and measurements of the amplitude of single-channel currents in the tails of synaptic responses. As shown in Figure 4, *A* and *B*, there was no change in the single-channel current of NMDA receptors after transfection with either NR2A or NR2B. Averaged data from nine cells led to a current measurement of 3.8 ± 0.6 pA (mean ± SD) for control and 3.8 ± 0.7 and 3.8 ± 0.6 pA for NR2A- and NR2B-transfected cells, respectively (see also Clark et al., 1997). Under these conditions the same kinetic changes were seen as recordings at +60 mV, with NR2A transfection producing faster and NR2B producing slower mEPSCs ($p < 0.01$). Furthermore, there was no detectable change in NMDA-mEPSC amplitude after the transfection of NR2 subunits as shown in Figure 4*D*, confirming results in neurons recorded at +60 mV.

Ifenprodil effects on NMDA-mEPSC recorded at −60 mV were studied in NR2-transfected or control CGCs. No significant change was seen with ifenprodil in average NMDA-mEPSC amplitude from any group of cells (in at least 7 cells in each group). In contrast, the reduction in mEPSC frequency in the presence of ifenprodil was significant for control CGCs and NR2B-transfected neurons (40 ± 11 and 58 ± 6%, respectively).

NR2 subunit expression does not control NMDA channel open probability in CGCs

The similar amplitude of NMDA-mEPSCs after transfection with either NR2A or NR2B was surprising in light of previous data indicating the higher probability of opening of NR2A-containing receptors in HEK 293 cells (Chen et al., 1999). Changes in peak open probability of the receptor would be expected to change the peak amplitude of the NMDA-mEPSC, but this amplitude was similar for control, NR2A-, and NR2B-transfected CGCs (Figs. 3, 4). To study possible changes in peak open probability, we pulled nucleated patches from CGCs, and we studied currents elicited by the fast application of 1 mM glutamate (4 msec application in the presence of 5 μM NBQX to block AMPA receptors in recording solution with 0.2 mM Ca^{2+} to decrease the rundown of response). There was high variability in the amplitude of response of these patches to glutamate, with a range from 30 to 1200 pA. This likely was related to differences in the size of the patch pulled, with some cases in which the whole cell body could be lifted from the coverslip. The kinetic difference between NR2B-transfected patches and control was statistically significant, but not that between NR2A and control (Fig. 5*B*). In all cases the kinetics of response were very similar to those seen for

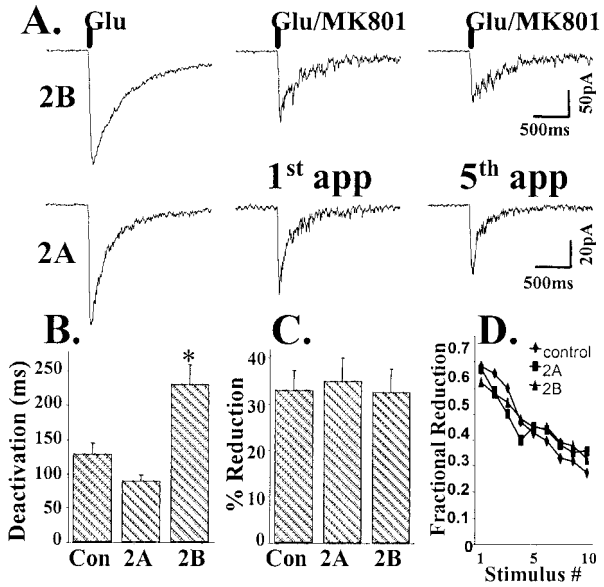

Figure 5. Progressive block of NMDA responses by MK-801. Nucleated patches were pulled from transfected or control CGCs and placed in the flow of a piezo-driven double-barrel pipette. Then 4 msec pulses from control solution (with 20 μM D-serine and 5 μM NBQX to block AMPA responses) to the same solution with 1 mM glutamate were applied to determine the baseline response, labeled in *A* as the glutamate response (*Glu*). Glutamate solution then was exchanged for a solution containing 1 mM glutamate and 20 μM MK-801 (*Glu/MK801*), which blocks NMDA channels that open during the 4 msec pulse of glutamate/MK-801. Responses to the repeated application of glutamate/MK-801 were recorded as shown in the traces in *A*. We measured the deactivation kinetics of glutamate alone (*B*), and transfection with the NR2B subunit showed a significant increase in the weighted time constant (τ_w; $^*p < 0.01$). *C*, The percentage of decrease in the amplitude of response to the first glutamate/MK-801 application compared with glutamate alone (responses from at least 8 patches in each group), which was not different for the different groups. *D*, The progressive block of NMDA responses with repeated MK-801 applications (*filled diamonds*, control; *filled squares*, NR2A; *filled triangles*, NR2B-transfected neurons; from at least 4 patches in each group).

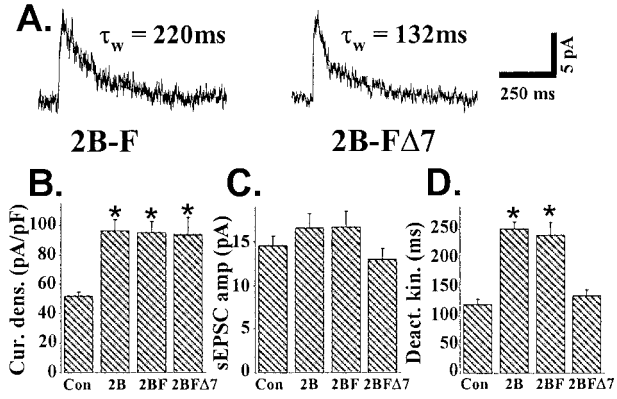

Figure 6. Functional analysis of the transfection of epitope-tagged NR2B-Flag and NR2B-FlagΔ7 in CGCs. Epitope-tagged constructs of NR2B-Flag and NR2B-FlagΔ7 (lacking the PDZ binding domain) were transfected into CGCs. *A*, Averaged synaptic traces from individual CGCs that were transfected with either NR2B-F or NR2B-FΔ7 (cultured in low K^+, as in Fig. 4). *B*, The current density of response to 200 μM NMDA with 20 μM D-serine applied via Y-tubing. The amplitude (*C*) and decay kinetics (*D*) of sEPSCs were measured as in Figure 3. At least seven cells were included in all groups. *Statistically significant from the value in control cells ($p < 0.05$).

the mEPSCs. After we recorded from successive glutamate applications until a steady baseline was seen, we switched the glutamate solution to a glutamate solution containing 20 μM MK-801, which will block only those receptors that bind glutamate and open during the brief agonist application. The amplitude decrease over a successive application of glutamate/MK-801 will depend on the duration of the application and the peak open probability of the receptor (Chen et al., 1999). The responses of an NR2A- and an NR2B-transfected CGC to glutamate and successive glutamate/MK-801 applications are shown in Figure 5*A*. Figure 5*C* shows quantification of the percentage of decrease of response in the first application of glutamate/MK-801 compared with glutamate alone, which was ~30% for each group (data from at least 7 cells in each group). Figure 5*D* shows progressive declining amplitude from patch currents that were recorded from a series of glutamate/MK-801 applications. This illustrates that there was no difference in the rate of decrease in amplitude of response after multiple applications with MK-801. From the third to ninth glutamate/MK-801 applications there was an ~10% decrease in current with each consecutive application for each group. The stronger block on the first pulse of glutamate/MK-801 likely indicates that there is a subpopulation of receptors with a significantly higher peak open probability that are blocked rapidly by the initial application and a second pool with a lower peak open probability that are blocked more slowly.

If a mixed receptor population with distinct kinetics and peak open probability were present in excised nucleated patches from transfected cells, one would expect that, by blocking the high open probability channels first, the kinetics of the low open probability channel would become predominant. In comparing the deactivation kinetics of response to glutamate alone versus glutamate/MK-801, we did not observe significant changes in the weighted time constant of deactivation (see traces in Fig. 5*A* over successive traces; at least 5 cells in each group). This implied that there were not kinetically distinct populations of channels that differed in peak open probability.

PDZ binding domain controls NR2B subunit targeting to the synapse

To study the effect of mutations of the C terminus of the NR2B subunit, we used a tagged NR2B construct (NR2B-Flag) with a Flag epitope inserted into the extracellular N terminus (Hawkins et al., 1999). From NR2B-Flag another construct was made with deletion of the last seven amino acids, including the PDZ interacting domain of NR2B (NR2B-FlagΔ7) that mediates interactions of the NMDA receptors with PSD-93, PSD-95, and SAP102 (for review, see Sheng, 2001). NR2B-Flag or NR2B-FlagΔ7 did not show surface staining when expressed alone in HEK 293 cells with the use of the Flag-specific antibody (similar to wild-type NR2A; McIlhinney et al., 1998), but surface expression of the NR2B-Flag and NR2B-FlagΔ7 was seen in HEK 293 cells cotransfected with NR1-1a and in transfected CGCs, indicating an ability to coassemble with endogenous NR1 subunits.

The current density after transfection was measured with applications of 200 μM NMDA with 1 μM TTX. With either NR2B-Flag or NR2B-FlagΔ7 transfections there was a significant increase in the current density ($p < 0.01$) of transfected CGCs compared with control cells, which was not different from the effect of NR2B transfection (Fig. 6*B*). The synaptic entry of receptors containing NR2B-Flag was seen in a significant increase in the τ_w of decay of the synaptic current, which was similar

to the effect of transfection with NR2B wild type (Fig. 6*A,D*; $p < 0.01$). These data indicate that the tagging of the receptor did not cause a change in the targeting or kinetics of the channel.

In comparison, after transfection with the NR2B-FlagΔ7 subunit there was no effect on the kinetics of the sEPSC compared with control CGCs (Fig. 6*D*). To exclude the possibility that the deletion of the PDZ binding domain caused a change in the deactivation kinetics of the channel, we performed control experiments with 4 msec applications of 1 mM glutamate with 10 μM glycine to HEK 293 cells that were transfected with NR1-1a and either NR2B-Flag or NR2B-FlagΔ7. The τ_w of deactivation to this glutamate pulse was 246 ± 51 msec for NR2B-Flag and 233 ± 11 msec for NR2B-FlagΔ7 ($n = 4$ for each). These values are similar to those published previously for wild-type NR2B (Cull-Candy et al., 2001) and are similar to the kinetics of the sEPSC in CGCs that were transfected with either wild-type NR2B or NR2B-Flag (Fig. 6*D*). Therefore, the lack of change in sEPSC kinetics after the overexpression of NR2B-FlagΔ7 is likely attributable to an inability of this subunit to be inserted into the pool of synaptic receptors.

DISCUSSION

In the present study we used the CGC system to investigate the delivery of NMDA receptors to the synapse. Our results show that the synaptic and total (which includes extrasynaptic receptors and receptors at both functional and nonfunctional synapses) pools of NMDARs are distinguished in two major ways: (1) the number of receptors in the synaptic pool is not affected significantly by increased synthesis of receptor complexes while the total pool is increased, and (2) the synaptic pool requires an interaction with a PDZ protein through the C terminus of the NR2B subunit. These results imply that neurons have a distinct mechanism for regulating the number of NMDARs at the synapse independently of subunit availability. In addition, whereas changes in NR2 subunit composition regulate ifenprodil sensitivity and mEPSC kinetics, the overexpression of NR2 subunits does not regulate the peak open probability of the receptors.

NR2 subunit expression determines the total number of functional receptors in CGCs

To study the effect of subunit overexpression, we measured whole-cell currents with the application of NMDA to CGCs. Although overexpression of the NR1 subunit did not affect the amplitude of NMDA-stimulated response significantly, the overexpression of either NR2A or NR2B caused a significant increase in the size of the response. Previous biochemical studies have indicated an intracellular pool of unassembled NR1 in CGCs, although most NR2A and NR2B subunit protein is present on the cell surface (Chazot and Stephenson, 1997; Huh and Wenthold, 1999). No change in total receptors was seen with the overexpression of NR1 splice variants that either contain the C1 cassette (NR1-1a, which is retained in the endoplasmic reticulum) or do not (NR1-4a). In addition, this effect of NR2 subunit overexpression also was seen in cortical neurons and in the absence of activity (CGCs in high K^+ media). These data also were supported by immunocytochemical analysis that showed a greater density of surface-labeled NR1 subunit clusters in CGCs that were cotransfected with either NR2A or NR2B compared with expression of tagged NR1 alone. Therefore, the total number of functional NMDA receptors is controlled by expression of the NR2 subunits, with a surplus of NR1 protein that lacks an NR2 subunit partner.

NMDA current densities do not relate solely to the number of functional channels expressed, but also to single-channel conductance, kinetics, and peak open probability. However, channels with NR2A or NR2B subunit in recombinant systems show similar single-channel conductance or open time (Stern et al., 1992). As more fully discussed later, we independently determined that the peak open probability did not change with NR2 subunit overexpression (Fig. 5). Therefore, the increase in current density after NR2 subunit overexpression is attributable to an increase in functional receptors. This indicates that strict control of NR2A and NR2B subunit protein is an important means for the cell to control excitability, whereas changes in expression of the NR1 are less likely to affect functional receptor number.

NR2 subunit overexpression changes the kinetics of synaptic sEPSCs, but not the number of receptors

Overexpression of the NR2A or NR2B subunit did not cause a significant change in the amplitude or frequency of the NMDA-mEPSCs, even with the increase in the number of receptors in the total receptor pool. Although central synapses might not be saturated (Mainen et al., 1999), a larger receptor pool at postsynaptic sites would increase the amplitude of response independently of whether the receptors were saturated. Therefore, postsynaptic changes in receptor number should be detectable independently of the concentration of glutamate released. The lack of change in NMDA-mEPSC amplitude or frequency thus argues that there is a mechanism controlling the number of NMDARs at functional synaptic sites. In addition, there was a decrease in the percentage of surface-labeled NR1 puncta colocalized with synaptophysin after the overexpression of either NR2A or NR2B, indicating that these new receptors are mainly at extrasynaptic sites. The finding that receptors formed after increased expression of NR2 subunits have a preference for extrasynaptic sites is especially interesting in light of recent data that extrasynaptic NMDA receptors are critical mediators of excitotoxic damage (Hardingham et al., 2002). In addition, these findings imply that there is a limited number of "slots" for synaptic NMDARs, that delivery of NMDARs to the synapse is limited by means besides subunit availability.

The kinetics of the NMDA-mEPSCs were determined by NR2 subunit overexpression. Previous biochemical (Sheng et al., 1994; Luo et al., 1997) and functional data (Stocca and Vicini, 1998; Tovar and Westbrook, 1999) implicated a role of heteromeric NMDA receptors of NR1/NR2A/NR2B subunits within a single receptor complex at the synapse. Our present data also support the idea that there is functional expression of both NR2A and NR2B at synapse (whether in a single or in separate protein complexes), because transfection of either subunit modified the deactivation kinetics of the NMDA-mEPSC toward the properties of the subunit in recombinant systems (Vicini et al., 1998). Changing NR2 subunit expression with transfection was also able to alter responses to the NR2B-selective antagonist ifenprodil, with overexpression of the NR2A subunit causing a loss of the ability of ifenprodil to decrease the frequency of NMDA-mEPSCs. This is likely attributable to the apparent dominant effect of the NR2A subunit in determining ifenprodil sensitivity (Tovar and Westbrook, 1999), with the decrease in NMDA-mEPSCs in control and NR2B-transfected neurons being attributable to a block of NR2B-dominated synapses. Knock-out studies in mice have shown that either NR2A or NR2B can be targeted effectively to the synapse in the absence of the other subunit (Kadotani et al., 1996; Tovar et al., 2000), and we also saw

successful trafficking of either subunit to the synapse as determined by the change in NMDA-mEPSC kinetics.

Subunit composition does not alter peak open probability of NMDA receptors

Although NMDA-mEPSC kinetics changed with overexpression of either NR2A or NR2B, there was no change in NMDA-mEPSC amplitude. Previous data in heterologous systems have shown that NR2A/NR1-1a channels have significantly greater peak open probability than NR2B/NR1-1a channels, which would predict a greater current amplitude of NR2A-dominated synapses (Chen et al., 1999). Patches from NR2A- and NR2B-transfected CGCs showed no indication of a difference in MK-801 blockade (Fig. 5). Furthermore, progressive MK-801/glutamate applications did not change deactivation kinetics, indicating that there was no correlation between deactivation kinetics and peak open probability within the receptor population. These data along with the lack of change in NMDA-mEPSC amplitude with the transfection of NR2A or NR2B argue that NMDA subunit composition in neurons does not control peak open probability. Many signaling molecules such as brain-derived neurotrophic factor (Levine and Kolb, 2000), protein kinase C (Xiong et al., 1998), and calmodulin (Ehlers et al., 1996) might regulate more strongly the peak open probability of NMDARs in neurons.

The PDZ binding domain controls NR2 subunit expression in the synaptic pool of receptors

The PDZ binding domain of the NR2 subunits mediates interactions with MAGUK proteins expressed at the postsynaptic density, including PSD-93, PSD-95, and SAP102 (for review, see Garner et al., 2000; Sheng, 2001; Tomita et al., 2001). Previous studies on transgenic mice (Mori et al., 1998; Sprengel et al., 1998; Steigerwald et al., 2000) showed that the C terminus of NR2 subunits is critical for localization of the NMDAR to the synapse. Because these mice lacked a large region of the NR2 C terminus, however, the specific role of the PDZ binding domain was not defined, because many additional sites are candidates to mediate the synaptic delivery and retention of the NMDAR. We therefore designed experiments to use the change in kinetics with NR2B overexpression as a marker for subunit incorporation into the synaptic pool of receptors. NR2B-FlagΔ7 (lacking the PDZ binding domain) overexpression had no effect on the deactivation kinetics of the NMDA-mEPSCs in comparison to the change seen with NR2B-Flag, although both increased the total number of functional receptors. This is consistent with a loss of PDZ-mediated stabilization of the receptor at the synapse leading to migration to extrasynaptic sites or increased endocytosis at synaptic sites. Loss of the PDZ binding domain has been shown to increase endocytosis of the NMDA NR2B C terminus (Roche et al., 2001). Another interesting possibility is that the PDZ binding domain plays a role early in the biosynthetic pathway and that synaptic and extrasynaptic pools are separated before reaching their final delivery site. It has been shown recently that the NR1 subunit with the C2′ cassette can interact through its PDZ binding domain while it is still in the endoplasmic reticulum (Standley et al., 2000; Scott et al., 2001). The GluR1 subunit of the AMPA receptor also associates with SAP97 while the complex is maturing in the endoplasmic reticulum (Sans et al., 2001). Thus a PDZ interaction early in the biosynthesis may be critical for synaptic delivery of receptor complexes.

REFERENCES

Chazot PL, Stephenson FA (1997) Biochemical evidence for the existence of a pool of unassembled C2 exon-containing NR1 subunits of the mammalian forebrain NMDA receptor. J Neurochem 68:507–516.

Chen C, Okayama H (1987) High-efficiency transformation of mammalian cells by plasmid DNA. Mol Cell Biol 7:2745–2752.

Chen L, Chetkovich DM, Petralia RS, Sweeney NT, Kawasaki Y, Wenthold RJ, Bredt DS, Nicoll RA (2000) Stargazin regulates synaptic targeting of AMPA receptors by two distinct mechanisms. Nature 408:936–943.

Chen N, Luo T, Raymond LA (1999) Subtype-dependence of NMDA receptor channel open probability. J Neurosci 19:6844–6854.

Clark BA, Farrant M, Cull-Candy SG (1997) A direct comparison of the single-channel properties of synaptic and extrasynaptic NMDA receptors. J Neurosci 17:107–116.

Corsi L, Li JH, Krueger KE, Wang YH, Wolfe BB, Vicini S (1998) Up-regulation of NR2B subunit of NMDA receptors in cerebellar granule neurons by Ca^{2+}/calmodulin kinase inhibitor KN93. J Neurochem 70:1898–1906.

Crump FT, Dillman KS, Craig AM (2001) cAMP-dependent protein kinase mediates activity-regulated synaptic targeting of NMDA receptors. J Neurosci 21:5079–5088.

Cull-Candy S, Brickley S, Farrant M (2001) NMDA receptor subunits: diversity, development, and disease. Curr Opin Neurobiol 11:327–335.

Dingledine R, Borges K, Bowie D, Traynelis SF (1999) The glutamate receptor ion channels. Pharmacol Rev 51:7–61.

Dunah AW, Standaert DG (2001) Dopamine D1 receptor-dependent trafficking of striatal NMDA glutamate receptors to the postsynaptic membrane. J Neurosci 21:5546–5558.

Ehlers MD, Zhang S, Bernhadt JP, Huganir RL (1996) Inactivation of NMDA receptors by direct interaction of calmodulin with the NR1 subunit. Cell 85:745–755.

Gallo V, Kingsbury A, Balazs R, Jorgensen OS (1987) The role of depolarization in the survival and differentiation of cerebellar granule cells in culture. J Neurosci 7:2203–2213.

Garner CC, Nash J, Huganir RL (2000) PDZ domains in synapse assembly and signaling. Trends Cell Biol 10:274–280.

Hardingham GE, Fukunaga Y, Bading H (2002) Extrasynaptic NMDARs oppose synaptic NMDARs by triggering CREB shut-off and cell death pathways. Nat Neurosci 5:405–414.

Hawkins LM, Chazot PL, Stephenson FA (1999) Biochemical evidence for the co-association of three *N*-methyl-D-aspartate (NMDA) R2 subunits in recombinant NMDA receptors. J Biol Chem 274:27211–27218.

Huh KH, Wenthold RJ (1999) Turnover analysis of glutamate receptors identifies a rapidly degraded pool of the *N*-methyl-D-aspartate receptor subunit, NR1, in cultured cerebellar granule cells. J Biol Chem 274:151–157.

Kadotani H, Hirano T, Masugi M, Nakamura K, Nakao K, Katsuki M, Nakanishi S (1996) Motor discoordination results from combined gene disruption of the NMDA receptor NR2A and NR2C subunits, but not from single disruption of the NR2A or NR2C subunit. J Neurosci 16:7859–7867.

Kennedy MB (1998) Signal transduction molecules at the glutamatergic postsynaptic membrane. Brain Res Brain Res Rev 26:243–257.

Lan JY, Skeberdis VA, Jover T, Grooms SY, Lin Y, Araneda RC, Zheng X, Bennett MV, Zukin RS (2001) Protein kinase C modulates NMDA receptor trafficking and gating. Nat Neurosci 4:382–390.

Levine ES, Kolb JE (2000) Brain-derived neurotrophic factor increases activity of NR2B-containing *N*-methyl-D-aspartate receptors in excised patches from hippocampal neurons. J Neurosci Res 62:357–362.

Luo J, Wang Y, Yasuda RP, Dunah AW, Wolfe BB (1997) The majority of *N*-methyl-D-aspartate receptor complexes in adult rat cerebral cortex contain at least three different subunits (NR1/NR2A/NR2B). Mol Pharmacol 51:79–86.

Mainen ZF, Malinow R, Svoboda K (1999) Synaptic calcium transients in single spines indicate that NMDA receptors are not saturated. Nature 399:151–155.

McIlhinney RA, Le Bourdelles B, Molnar E, Tricaud N, Streit P, Whiting PJ (1998) Assembly, intracellular targeting, and cell surface expression of the human *N*-methyl-D-aspartate receptor subunits NR1a and NR2A in transfected cells. Neuropharmacology 37:1355–1367.

Mellor JR, Merlo D, Jones A, Wisden W, Randall AD (1998) Mouse cerebellar granule cell differentiation: electrical activity regulates the $GABA_A$ receptor 6 subunit gene. J Neurosci 18:2822–2833.

Mori H, Manabe T, Watanabe M, Satoh Y, Suzuki N, Toki S, Nakamura K, Yagi T, Kushiya E, Takahashi T, Inoue Y, Sakimura K, Mishina M (1998) Role of the carboxy-terminal region of the GluR ε2 subunit in synaptic localization of the NMDA receptor channel. Neuron 21:571–580.

Murase K, Ryu PD, Randic M (1989) Excitatory and inhibitory amino acids and peptide-induced responses in acutely isolated rat spinal dorsal horn neurons. Neurosci Lett 103:56–63.

Roche KW, Standley S, McCallum J, Dune Ly C, Ehlers MD, Wenthold

RJ (2001) Molecular determinants of NMDA receptor internalization. Nat Neurosci 4:794–802.
Rumbaugh G, Vicini S (1999) Distinct synaptic and extrasynaptic NMDA receptors in developing cerebellar granule neurons. J Neurosci 19:10603–10610.
Sans N, Racca C, Petralia RS, Wang YX, McCallum J, Wenthold RJ (2001) Synapse-associated protein 97 selectively associates with a subset of AMPA receptors early in their biosynthetic pathway. J Neurosci 21:7506–7516.
Scott DB, Blanpied TA, Swanson GT, Zhang C, Ehlers MD (2001) An NMDA receptor ER retention signal regulated by phosphorylation and alternative splicing. J Neurosci 21:3063–3072.
Sheng M (2001) Molecular organization of the postsynaptic specialization. Proc Natl Acad Sci USA 98:7058–7061.
Sheng M, Cummings J, Roldan LA, Jan YN, Jan LY (1994) Changing subunit composition of heteromeric NMDA receptors during development of rat cortex. Nature 368:144–147.
Sinor JD, Du S, Venneti S, Blitzblau RC, Leskiewicz DN, Rosenberg PA, Aizenmann E (2000) NMDA and glutamate evoke excitotoxicity at distinct cellular locations in rat cortical neurons *in vitro*. J Neurosci 20:8831–8837.
Sprengel R, Suchanek B, Amico C, Brusa R, Burnashev N, Rozov A, Hvalby O, Jensen V, Paulsen O, Andersen P, Kim JJ, Thompson RF, Sun W, Webster LC, Grant SG, Eilers J, Konnerth A, Li J, McNamara JO, Seeburg PH (1998) Importance of the intracellular domain of NR2 subunits for NMDA receptor function *in vivo*. Cell 92:279–289.
Standley S, Roche KW, McCallum J, Sans N, Wenthold RJ (2000) PDZ domain suppression of an ER retention signal in NMDA receptor NR1 splice variants. Neuron 28:887–898.
Steigerwald F, Shulz TW, Schenker LT, Kennedy MB, Seeburg PH, Kohr G (2000) C-terminal truncation of NR2A subunits impairs synaptic but not extrasynaptic localization of NMDA receptors. J Neurosci 20:4573–4581.
Stern P, Behe P, Schoepfer R, Colquhoun D (1992) Single-channel conductances of NMDA receptors expressed from cloned cDNAs: comparison with native receptors. Proc R Soc Lond B Biol Sci 250:271–277.
Stocca G, Vicini S (1998) Increased contribution of NR2A subunit to synaptic NMDA receptors in developing rat cortical neurons. J Physiol (Lond) 507:13–24.
Tomita S, Nicoll RA, Bredt DS (2001) PDZ protein interactions regulating glutamate receptor function and plasticity. J Cell Biol 153: F19–F24.
Tovar KR, Westbrook GL (1999) The incorporation of NMDA receptors with a distinct subunit composition at nascent hippocampal synapses *in vitro*. J Neurosci 19:4180–4188.
Tovar KR, Westbrook GL (2002) Mobile NMDA receptors at hippocampal synapses. Neuron 34:255–264.
Tovar KR, Sprouffske K, Westbrook GL (2000) Fast NMDA receptor-mediated synaptic currents in neurons from mice lacking the $\epsilon 2$ (NR2B) subunit. J Neurophysiol 83:616–620.
Vicini S, Wang JF, Li JH, Zhu WJ, Wang YH, Luo JH, Wolfe BB, Grayson DR (1998) Functional and pharmacological differences between recombinant *N*-methyl-D-aspartate receptors. J Neurophysiol 79:555–566.
Vissel B, Krupp JJ, Heinemann SF, Westbrook GL (2001) A use-dependent tyrosine dephosphorylation of NMDA receptors is independent of ion flux. Nat Neurosci 4:587–596.
Williams K (1993) Ifenprodil discriminates subtypes of the *N*-methyl-D-aspartate receptor: selectivity and mechanisms at recombinant heteromeric receptors. Mol Pharmacol 44:851–859.
Xiong ZG, Raouf R, Lu WY, Wang LY, Orser BA, Dudek EM, Browning MD, MacDonald JF (1998) Regulation of *N*-methyl-D-aspartate receptor function by constitutively active protein kinase C. Mol Pharmacol 54:1055–1063.